JOURNAL OF CATALYSIS **169,** 438–446 (1997)
ARTICLE NO. CA971725

Reaction and Surface Characterization Study of Higher Alcohol Synthesis Catalysts

I. K-Promoted Commercial Zn/Cr Spinel

William S. Epling,* Gar B. Hoflund,* Walter M. Hart,† and David M. Minahan†

*Department of Chemical Engineering, University of Florida, Gainesville, Florida 32611; and †Union Carbide Corporation, Technical Center/P.O. Box 8361, South Charleston, West Virginia 25303

Received September 20, 1996; revised April 14, 1997; accepted April 17, 1997

A commercial Zn/Cr spinel methanol synthesis catalyst obtained from Engelhard was promoted with potassium and tested for methanol and isobutanol synthesis using a syngas feedstream (1 : 1 H_2 and CO). An equal molar mixture of methanol and isobutanol would be an ideal feedstock for production of methyl tertiary butyl ether (MTBE) for use as an additive to gasoline to increase the octane number and reduce air pollution. Of the reaction conditions examined, the higher temperature, 440°C, and higher pressure, 1500 psig, result in the highest isobutanol production rate over most of the catalysts examined. The effect of the K promotor loading also was examined. Increasing the amount of K from 0 to 1 wt% increases the hydrocarbon by-product rate, but the addition of 3 or 5 wt% K decreases the hydrocarbon by-product rate consequently increasing the selectivity to total alcohols. Increasing the K loading above 3 wt%, however, raises the methanol-to-isobutanol mole ratio. The use of the 3 wt% K-containing catalyst results in the lowest methanol-to-isobutanol mole ratio of 1.5 which is near the desired value of 1.0 for MTBE synthesis. An isobutanol production rate of 103 g/kg-cat/hr is attained using a 1 wt% K-promoted Zn/Cr spinel catalyst. Surface-characterization studies were performed on the 3 wt% K-containing catalyst. Ion-scattering spectroscopy data reveal that the outermost surface layer of the fresh catalyst consists of C, O, Cr, and Zn. Since the catalysts are reduced prior to testing in the reactor, surface studies also were performed after reducing the catalyst in 1×10^{-7} Torr of H_2 for 4 hr at 250°C. The addition of the alkali is necessary for higher alcohol synthesis (HAS), and the pretreatment results in migration of the K promotor to the outermost surface layer where the catalytic reactions occur. X-ray photoelectron spectroscopy (XPS) data are consistent with these results and also reveal that the near-surface regions of the nontreated and H_2-treated samples consist primarily of ZnO. The K is present as $K_2Cr_2O_7$ or K_2CrO_4. Although the outermost atomic layer of the reduced catalyst contains a large amount of K, relatively little is observed in the near-surface region using XPS, indicating that most of the K is located at the surface. The catalytically active surface for HAS consists of alkali species lying on top of a ZnO phase. The chemical state of the Cr species is altered during reaction. The $K_2Cr_2O_7$ or K_2CrO_4 present on the fresh and reduced catalyst is converted to Cr_2O_3, $Cr(OH)_x$ and Cr^0 with age, but no other phases of Zn other than ZnO are observable before or after aging. The Zn/Cr spinel is not important for activity toward isobutanol production and acts only as a high-surface-area support. © 1997 Academic Press

INTRODUCTION

During the past 10 years, there has been considerable interest in developing processes for the synthesis of higher alcohols (C_2 and higher) from syngas for use as additives to gasoline (usually 2–5 wt%) to reduce air pollution and increase the octane number (1). The need for an octane enhancer stems from the phasing out of lead from the gasoline pool and a push for higher levels of pollution control. The presence of oxygen in the fuel allows for combustion to proceed to a greater extent, thus lowering the amount of hydrocarbon emissions. Higher alcohols are useful as additives to gasoline or substitute fuels such as methanol. For example, combining a mixture of C_2–C_5 alcohols with methanol helps overcome the problem of methanol phase separation with water and lowers the overall vapor pressure of the methanol fuel. An alcohol mixture produced from syngas could be added to the list of (or be used to synthesize) such established octane improvers such as methyl tertiary butyl ether (MTBE), ethyl tertiary butyl ether, and tertiary amyl methyl ether or be used directly as are alcohols such as methanol, ethanol, and tertiary butyl alcohol. Besides their value as a source of acceptable octane enhancers, processes for producing a mixture of alcohols from syngas could be of particular interest for the conversion of remote natural gas to easily transportable, high-value products (2). A 50/50 mol% mix of methanol and isobutanol would provide an ideal feedstock for the direct production of methyl isobutyl ether (MIBE) via dehydration or the indirect production of MTBE in two steps by (a) dehydration of the isobutanol to isobutylene, followed by (b) reaction with methanol to produce MTBE. The second route

0021-9517/97 $25.00

is preferred because MIBE is not an octane-enhancing agent.

Catalysts for higher alcohol synthesis (HAS) can be divided into the following two classes (3) based on the alcohol product distribution. One is modified Fischer–Tropsch (FT) and the other is Group VIII metal-based catalysts.

Traditional Fischer–Tropsch catalysts produce appreciable amounts of oxygenates (alcohols, aldehydes, acids, ketones, and esters) by addition of alkali. The products obtained follow an Anderson–Schultz–Flory (ASF) distribution, typical of the well-known linear condensation polymerization mechanism. Molybdenum sulfide catalysts promoted with alkali also produce the ASF product distribution while Rh-based catalysts are similar but produce more C_{2+} oxygenates.

HAS catalysts have evolved primarily from modified methanol-synthesis catalysts. The original methanol synthesis catalysts were based on a Zn/Cr spinel. A second catalyst type which operates at substantially lower temperatures (250–300°C) is composed of a Cu–metal-based formulation. In both cases the addition of alkali to the systems results in the formation of higher alcohols, albeit at a substantially lower overall productivity. The reaction is believed to proceed by a combination of hydrogenation and carbon–carbon bond formation via aldol condensation. This is in contrast to the modified FT catalysts which function through a classical CO insertion/hydrogenation mechanism. The result of this is the formation of branched alcohols with a non-ASF product distribution. The following major reactions take place over the catalyst:

Alcohol formation

$$n\mathrm{CO} + 2n\mathrm{H_2} \rightarrow \mathrm{C}_n\mathrm{H}_{2n+1}\mathrm{OH} + (n-1)\mathrm{H_2O}$$

Hydrocarbon formation

$$n\mathrm{CO} + (2n+1)\mathrm{H_2} \rightarrow \mathrm{C}_n\mathrm{H}_{2n+2} + n\mathrm{H_2O}$$

Water–gas-shift reaction equilibrium

$$\mathrm{CO} + \mathrm{H_2O} \rightleftarrows \mathrm{CO_2} + \mathrm{H_2}$$

The formation of methanol and isobutanol with the addition of Cs or K to the copper-based catalysts has been studied extensively (3–11). The alcohol distribution obtained using these catalysts, however, is undesirable thus far for the direct product application of MTBE synthesis because the methanol-to-isobutanol mole ratio is too large. Furthermore, significant quantities of by-products are produced and long contact times are necessary. In some cases the reaction conditions result in catalyst instability possibly due to catalyst sintering (12, 13). The alkali promotion of the zinc–chromite catalysts also results in higher alcohol production (3, 12–16). Less attention has been given to these catalysts because more severe reaction conditions are required. Nevertheless, upon K addition the primary alcohol formed using these catalysts is isobutanol. Again, however, a larger amount of methanol is produced resulting in a poor alcohol distribution. The advantage of these catalysts is that better selectivities for isobutanol production are achieved compared to the Cu-based catalysts. Beretta *et al.* (15) recently examined the use of the two types of catalysts in series and achieved a productivity of 138.8 g/kg-hr of isobutanol and a methanol-to-isobutanol mole ratio of 3. These values are the most promising published in the literature, and the qualities of these catalysts may be enhanced further through the use of reaction engineering. As noted above, the detailed optimization of the zinc–chromite catalysts has not been extensively examined or achieved.

The present study is the first of a series which focuses on the optimization of isobutanol synthesis using modified high-temperature, high-pressure methanol-synthesis catalysts. The goal is to achieve a high production rate of isobutanol, a methanol-to-isobutanol mole ratio of 1.0, and a low hydrocarbon production rate. A commercially available Zn/Cr spinel methanol-synthesis catalyst, Engelhard Zn-0312, which has been promoted with varying amounts of K has been examined for HAS in this investigation. Reaction studies were performed using each of the K-promoted Zn/Cr spinel catalysts made in order to determine the optimum promotor concentration and preferred operating conditions. X-ray photoelectron spectroscopy (XPS) and ion-scattering spectroscopy (ISS) were used to examine the fresh, pretreated, and aged catalyst surfaces before and after sputtering in order to relate compositional and chemical-state information regarding the near-surface region of the catalyst to the catalytic behavior. This approach leads to a novel insight regarding how these catalysts function.

EXPERIMENTAL

Reaction Studies

The Zn/Cr spinel support was purchased from Engelhard Industries (Engelhard Zn-0312). The bulk Zn-to-Cr weight ratio is this spinel is 3:1, and the O content is 21 wt%. The catalysts were impregnated with 1, 3, and 5 wt% K as a promotor using potassium nitrate and the incipient wetness method. The reactor consisted of a $\frac{1}{4}$-in. copper tube inserted into a $\frac{3}{8}$-in. stainless-steel tube. This arrangement eliminates products which form due to feedstream reactions with the stainless steel at the elevated temperatures. One gram of catalyst powder was mixed with 3 g of glass beads for catalyst dispersion and then placed into the reactor tubes. These tubes were placed into an air fluidized sandbath which was used for heating uniformly. The feed and pretreatment gases were passed through a molecular-sieve-activated carbon trap to remove water and metal carbonyl contaminants before entering the reactor tube. The catalysts were calcined in air at 325°C to stabilize the

material and then reduced with a 5% hydrogen-in-nitrogen mixture for 4 hr at 300°C. The reactions were run using a feed gas of 1 : 1 H_2 and CO mixture at a space velocity of 12,000. The reactions were run at two different temperatures, 400 and 440°C, and pressures, 1000 (6.9 MPa) and 1500 psig (10.3 MPa). The product stream was analyzed using a Varian 3700 gas chromatograph. Inorganics were detected by thermal conductivity measurements using a Carbosieve S-2 column purchased from Supelco. The organic products were detected using a 12-ft, $\frac{1}{8}$-in., 80/100 Tenax column obtained from Alltech and detected using flame ionization. The Tenax column was calibrated on an absolute weight basis using quantified mixtures of C_1–C_6 normal hydrocarbons, normal and branched alcohols, and normal aldehydes. Separation of branched and primary alcohols was therefore attained. The focus of this study was the synthesis of isobutanol and therefore not all components of the product steam are mentioned, although residual alcohols can be determined from the remainder of the total alcohol rate. Argon was used as the carrier gas in both columns. Carbon mass balances were performed throughout the experiments by comparing the feed and product stream compositions using the gas chromatograph system. In some cases other oxygenates were detected but at levels in the 1 to 2% ranges.

Characterization Studies

The fresh catalyst material (unreacted) was pressed into an Al cup and inserted into an ultrahigh vacuum chamber (base pressure of $<10^{-10}$ Torr) to carry out the surface characterization studies. XPS and ISS data were collected using a double-pass cylindrical mirror analyzer (CMA) (PHI Model 15-255 GAR). XPS data were collected by operating the CMA in the retarding mode with pass energies set at 25 eV for the high-resolution spectra and 50 eV for the survey spectra. A Mg $K\alpha$ X-ray generator was used as the excitation source. Binding energy (BE) values were determined by assigning the Fermi level to 0.0 eV and then ensuring the Zn 2*p* peak of ZnO has a BE value of 1021.7 eV (17). ISS was performed using 1-keV He^+ defocused over a spot size of 0.5 cm^2. A total-ion current of 100 nA was used, and each spectrum was collected in 66 sec. The collection of an ISS spectrum using He^+ and the selected operating parameters results in the sputter removal of less than one-tenth of a monolayer. ISS spectra were collected by operating the CMA in the nonretarding mode and both XPS and ISS data were collected using pulse-counting detection (18).

After the initial surface characterization was accomplished, the fresh catalyst was reduced for 4 hr in 1×10^{-7} Torr of flowing research-grade H_2. The temperature was ramped at approximately 2°C per minute to 250°C and held at this temperature for the remaining time. The pretreated catalyst was then reanalyzed using XPS and ISS without exposure to air after the pretreatment. A depth profile was obtained by sputtering the sample with a 1-keV flux of 1 : 1 He^+ and Ar^+ for varying intervals of time while ISS spectra were collected. XPS again was used to examine the chemical states of the species present after sputtering. The aged catalysts were retrieved from the reactor after functioning for about 1 week under reaction conditions. These samples also were characterized using XPS, ISS, and depth profiling.

RESULTS AND DISCUSSION

A detailed listing of the product distribution using a nonpromoted and 1, 3, and 5 wt% K-promoted catalysts under four sets of reaction conditions is shown in Table 1. Since the highest isobutanol production rates and lowest methanol-to-isobutanol mole ratios are attained using a pressure of 1500 psi and 440°C for each catalyst except the 5 wt% K-containing sample, these seem to be the most favorable conditions of the four tested. The higher temperature, however, results in a loss of selectivity due to a higher hydrocarbon product rate. The higher pressure slightly increases the selectivity of the nonpromoted and 5 wt% K-containing catalyst and significantly increases the overall product rates over each of the catalysts. Small amounts of other alcohols also are produced, but isobutanol and methanol are consistently the primary products. The product stream composition obtained using the 3 wt% K catalyst at 400°C and 1000 psi as a function of time is given in Table 2. Little variation is noticeable after 15 hr on stream, and no trends in the product rates are evident other than the formation of *n*-propanol after 13 hr. Each catalyst was tested at each of the four operating parameters listed for a minimum of 24 hr. No significant changes in catalyst activity or product stream compositions were noted under any of the conditions tested.

The total alcohol production rate as a function of K loading at 440°C and 1500 psi is shown in Fig. 1a. The use of the 1 wt% K-containing catalyst results in the highest alcohol production rate. The nonpromoted catalyst produces significant quantities of alcohols, but the product stream is composed primarily of methanol and very little isobutanol as shown in Fig. 1b. The total alcohol production rate increases initially upon the addition of K but decreases to 99 g/kg-hr with the addition of 3 wt% K to the spinel and increases again to 130 g/kg-hr upon addition of 5 wt% K. The addition of K increases the isobutanol rate, and a maximum in production is achieved with the 1 wt%-K catalyst. A product stream flowrate of 103 g/kg-cat/hr of isobutanol is greater than that attained by Beretta *et al.* (15) using a $Cs/ZnO/Cr_2O_3$ catalyst. This catalyst yields a methanol-to-isobutanol mole ratio of 1.9, while an even lower ratio of 1.5 is achieved using the 3 wt% K catalyst. The effect of the addition of K on the selectivity to total alcohols is shown in Fig. 2a. The highest selectivity to total alcohols is attained using the 5 wt% K catalyst and decreases as the K loading decreases. The use of the nonpromoted catalyst results

TABLE 1

Catalytic Performance of the Zn/Cr Engelhard Spinel Containing

	0% K				1% K				3% K				5% K			
P (psig):	1000	1500	1500	1000	1000	1500	1500	1000	1000	1500	1500	1000	1000	1500	1500	1000
T (°C):	400	400	440	440	400	400	440	440	400	400	440	440	400	400	440	440
Selectivity to total alcohols (%)	65	77	43	27	61	75	53	53	80	88	70	70	96	97	84	83
Total alcohol rate (g/kg-hr)	111	236	133	59	133	251	167	129	75	159	99	67	82	159	130	70
Methanol rate (g/kg-hr)	105	223	102	41	78	170	49	70	38	92	26	8	59	123	47	16
Ethanol rate (g/kg-hr)	0	0	0	0	0	0	0	0	0	0	0	0	0	0	0	0
Isopropanol rate (g/kg-hr)	0	0	0	3	0	0	6	5	0	1	6	2	0	1	9	5
n-Propanol rate (g/kg-hr)	0	0	18	10	8	0	9	6	4	10	0	0	0	0	23	10
Isobutanol rate (g/kg-hr)	6	13	13	5	47	81	103	47	34	57	67	57	23	34	51	38
MetOH/i-ButOH mole ratio	73	68	31	36	6.6	8.4	1.9	6.0	4.5	6.4	1.5	0.54	10	14	3.7	1.7
Hydrocarbon rate (g/kg-hr)	30	35	94	86	48	46	101	65	11	12	29	21	2	3	15	10
Conversion (%)	8	14	14	9	12	19	19	13	10	12	13	11	13	14	15	13

in the lowest selectivity of 43%. As shown in Fig. 2b, the addition of 1 wt% K to the Zn/Cr spinel slightly increases the formation of hydrocarbon by-products. Increasing the amounts of K further results in a decrease in the amount of hydrocarbons produced which accounts for the increase in alcohol selectivity observed in Fig. 2a. Surface science analysis was performed on the Zn/Cr spinel catalyst containing 3 wt% K due to its low methanol-to-isobutanol mole ratio under the reaction conditions used.

ISS is an important surface science technique (19–22) in catalysis due to its extremely high surface sensitivity. Unlike AES and XPS this technique yields compositional information about the outermost atomic layer, which is where catalysis occurs. An ISS spectrum taken from the fresh 3 wt% K-promoted catalyst is shown in Fig. 3a. A predominant

TABLE 2

Product Stream Analysis Obtained Using the Zn/Cr Engelhard Commercial Spinel Support Plus 3 wt% K at 400°C and 1000 psig as a Function of Time

	Time on stream (hr)						
	3	5	7	9	11	13	15
Sel. total alcohols (%)	78	80	79	77	76	79	80
Total alcohol rate (g/kg-hr)	70	77	76	67	65	76	75
Methanol rate (g/kg-hr)	33	37	38	40	40	39	38
Ethanol rate (g/kg-hr)	0	0	0	0	0	0	0
Isopropanol rate (g/kg-hr)	0	0	0	0	0	0	0
n-Propanol rate (g/kg-hr)	0	0	0	0	0	4	4
Isobutanol rate (g/kg-hr)	36	40	38	27	25	33	34
MeOH/i-ButOH mole ratio	3.7	3.8	4.0	5.8	6.3	4.7	4.5
Hydrocarbon rate (g/kg-hr)	12	12	12	11	11	12	11
Conversion (%)	10	10	10	10	10	10	10

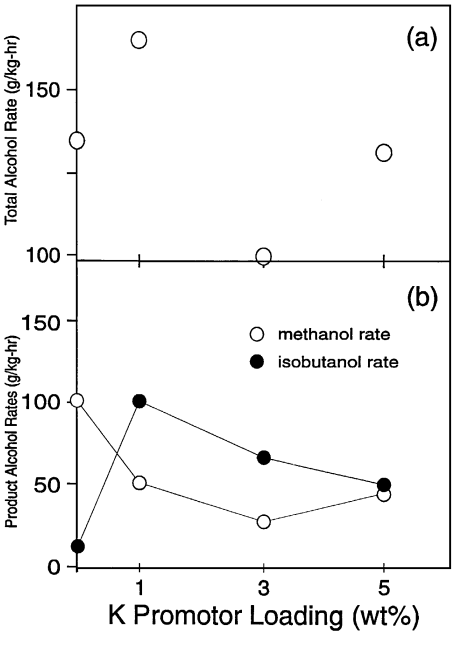

FIG. 1. The effect of K loading on (a) the total alcohol production rate and (b) the isobutanol and methanol production rates of the product stream when the reactor is operated at 440°C and 1500 psig.

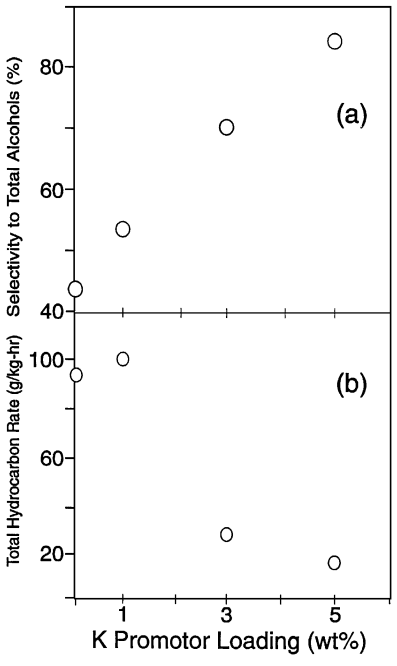

FIG. 2. The effect of K loading on (a) the selectivity to total alcohols (calculated on a mass basis) and (b) the total hydrocarbon production rate when the reactor is operated at 440°C and 1500 psig.

feature due to charging is present at an E/E_0 of 0.46. Features due to O and C also are apparent at E/E_0s of 0.38 and 0.27, respectively. Upon expanding the higher E/E_0 region by a factor of 5, Cr and Zn peaks become evident. This spectrum indicates that the as-prepared catalyst surface contains mostly O in the outermost atomic layer. The charging feature which is present in these spectra is most likely caused by the presence of large amounts of O at the surface. This results in an insulating surface layer which often leads to the observed charging features. Features due to charging typically are present in the lower E/E_0 portions of ISS spectra and therefore may influence the C and O peak positions, shapes, and intensities. The features due to heavier elements lie at higher E/E_0 values so these features are less affected by charging features. However, they may appear as small peaks due to the large size of the charging peak. After exposing the catalyst to 1×10^{-7} Torr of H_2 for 4 hr at 250°C, the ISS spectrum shown in Fig. 3b was taken. This treatment is similar to the pretreatment conditions used on the catalysts before they are exposed to the reaction stream. The charging feature is still large, but it appears at a lower E/E_0. One of the peaks in this charging feature such as the large peak at an E/E_0 of 0.32 may be due to O. Many variables affect the peak shapes and positions of the charging features, and as of yet no research has been accomplished on the development of models for understanding these features. After the reductive treatment the K peak is quite prominent, and the Zn and Cr peaks are not evident. The H_2 treatment may remove some surface O exposing underlying K and/or possibly some K may migrate to the surface covering the underlying Zn and Cr. The ISS spectrum shown in Fig. 3c was taken after the catalyst was sputtered with 1 keV He^+ for 5 min. A significant Zn feature is now evident indicating that the sputtering process removes some K from the surface, exposing a small amount of Zn located beneath the K layer. The low E/E_0 feature is similar in shape to that shown in Fig. 3b, but it is smaller relative to the higher E/E_0 features indicating that surface O has been selectively sputtered away. Another ISS spectrum shown in Fig. 3d was taken after sputtering the sample for 15 min with a 1-keV 1:1 He^+ and Ar^+ mixture. Most of the K layer has been sputtered away, the primary feature is due to Zn, a smaller Cr feature is evident and a feature due to Na contamination initially below the surface is also apparent. The low E/E_0 feature is reduced further in size relative to the higher E/E_0 features indicating further removal of surface O. Its position and shape are also changed. This probably is due to the fact that the surface composition is quite different after this sputter treatment so that the charging characteristics are altered.

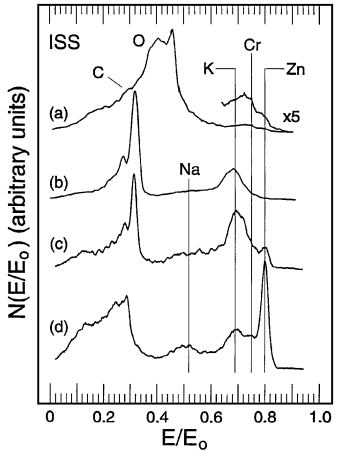

FIG. 3. ISS spectra taken from the 3 wt% K/Zn/Cr spinel catalyst after (a) insertion into the UHV system, (b) pretreating in 1×10^{-7} Torr of H_2 for 4 hr at 250°C, (c) sputtering for 5 min with 1 keV He^+, and (d) sputtering for another 15 min with a 1-keV 1:1 He^+ and Ar^+ mixture.

Surface analysis was performed on the aged catalysts after they had been in the reactor for about 5 days. The reaction data did not vary over this time period unless the operating parameters were adjusted to test another setting so the catalytic properties of these samples remain stable with time during the intervals used. An ISS spectrum taken from the aged 3-wt% K-promoted Zn/Cr spinel catalyst is shown in Fig. 4a. The outermost surface layer is significantly different from those of the as-prepared and pretreated catalysts. Features due to K, Cr, and Zn are all present, and a large Na peak is evident also. This indicates that the Na which is present in the near-surface region, but not at the surface, of

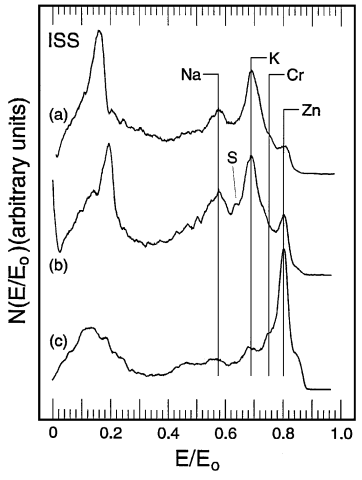

FIG. 4. ISS spectra taken from the aged 3 wt% K/Zn/Cr spinel catalyst after (a) insertion into the UHV system, (b) sputtering for 5 min with 1 keV He^+, and (c) sputtering for another 15 min with a 1-keV 1 : 1 He^+ and Ar^+ mixture.

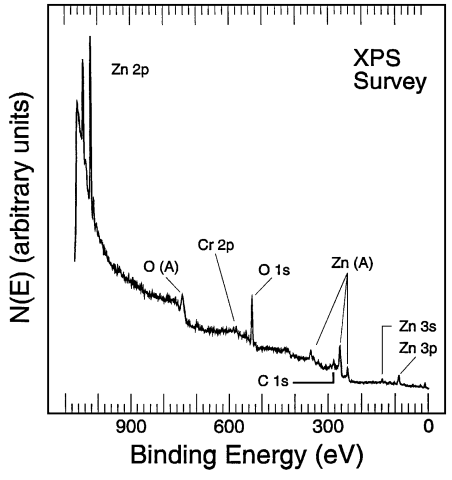

FIG. 5. XPS survey spectrum taken from the nonreacted, nonpretreated, 3 wt% K/Zn/Cr spinel catalyst.

the pretreated sample migrates toward the surface of the sample as the reaction proceeds or that the K may have agglomerated during reaction exposing the underlying Zn, Cr, and Na. The low E/E_0 feature is similar in shape to those in Figs. 3b and 3c, but it is shifted to lower E/E_0 and is reduced in size relative to the higher E/E_0 features indicating that less O is present on this surface. Sputtering the sample results in an increase in the surface Zn concentration relative to the K concentration as seen in Fig. 4b. The O concentration is reduced further, and the low E/E_0 feature is more similar in shape and position to those shown in Figs. 3b and 3c. A small peak at an E/E_0 of approximately 0.64 is caused by the presence of S contamination at the surface. The ISS spectrum shown in Fig. 4c was taken after sputtering the sample for an additional 15 min with a 1-keV 1 : 1 He^+ and Ar^+ mixture. Most of the K and Na is removed by the sputter process indicating that these species lie near the surface. The charging feature is reduced in size, and the spectrum is similar to one obtained from a bare spinel surface. A previous study reported that the O/Ag ISS cross section ratio is 0.05 (23). Although Zn is less massive than Ag, this value implies that the presence of even small O peaks represents significant amounts of O in the outermost atomic layer. The higher lying features due to the heavier elements are less affected by the charging as observed previously (24). The primary peak in this spectrum is due to Zn while a small shoulder due to Cr is present as well. This spectrum also is similar to that shown in Fig. 3d.

An XPS survey spectrum taken from the fresh catalyst is shown in Fig. 5. Predominant peaks due to Zn and O are readily apparent, and small Cr and C features also are present. The Cr features are much smaller than the Zn features indicating that the near-surface region of the catalyst is enriched in Zn with only a trace amount of Cr present. The carbon is a contaminant formed by exposure to air. Similar survey spectra were obtained from the reduced and aged catalysts and therefore are not presented. The most significant difference in the survey spectra is that the Cr 2*p* peaks are larger by a factor of about 2 after reduction of the fresh catalyst, are larger by a factor of about 3 for the aged catalyst, and doubled again after sputtering the aged catalyst.

-1A high-resolution XPS Zn 2*p* spectrum taken from the fresh catalyst is shown in Fig. 6a. ZnO appears to be the only chemical state of Zn present in the near-surface region (17). In fact, ZnO is the primary or only state of Zn present

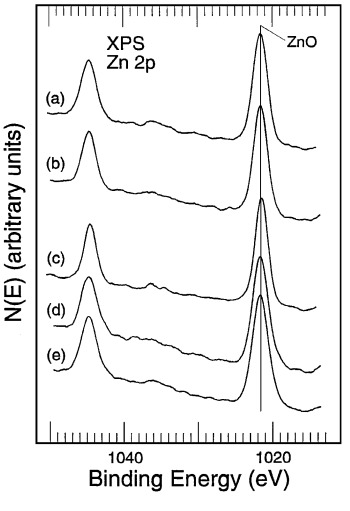

FIG. 6. XPS Zn 2*p* spectra taken from the 3 wt% K/Zn/Cr spinel catalyst after (a) insertion into the UHV system, (b) pretreating in 1×10^{-7} Torr of H_2 for 4 hr at 250°C, (c) sputtering for 5 min with 1 keV He^+ and 15 min with a 1-keV 1 : 1 He^+ and Ar^+ mixture, (d) the aged 3 wt% K/Zn/Cr spinel catalyst, and (e) the aged catalyst after sputtering for 5 min with 1 keV He^+ and 15 min with a 1-keV 1 : 1 He^+ and Ar^+ mixture.

in the near-surface region of all the catalyst surfaces examined (Figs. 6a–6e) in this study. An interaction between Cu and Zn produces a peak with a BE value which is 0.7 eV less than that of ZnO (25). A similar shift may occur if a Cr–Zn alloy were present, but no such feature is noticeable. Also a feature at 1022.1 eV due to $ZnCr_2O_4$ (26) is not apparent. The FWHM of all the Zn 2*p* features in Fig. 6 are similar as are their peak shapes. This supports the assertion that only one chemical state of Zn such as ZnO is present. These data also indicate that the Zn/Cr spinel does not play an active role in the catalytic process in HAS since no Zn–Cr spinel features are evident. The reaction process seems not to be based on the presence of the spinel structure or Cr.

A high-resolution XPS O 1*s* spectrum taken from the fresh catalyst is shown in Fig. 7a. The broad peak width indicates that a mixture of chemical states is present. ZnO and hydroxyl groups are the primary contributors to this signal. A small amount of adsorbed water as well as some chemisorbed O are also present. The assignment of this low BE feature is based on previous studies of the thermal decomposition of silver oxides (27, 28). After reducing the sample, the O 1*s* spectrum shown in Fig. 7b was taken. The contribution from OH is greatly diminished, but a small, well-defined shoulder due to adsorbed H_2O is apparent. The removal of the OH groups contributes to the exposure of more of the ZnO and possibly more catalytic sites. Sputtering the sample does not alter the O 1*s* peak significantly, as shown in Fig. 6c, but the adsorbed H_2O peak size is reduced. The O 1*s* spectrum taken from the aged catalyst is shown in Fig. 6d. Significant changes have occurred due to the reaction process. The primary feature still is assigned to ZnO, but the size of the chemisorbed O feature is now

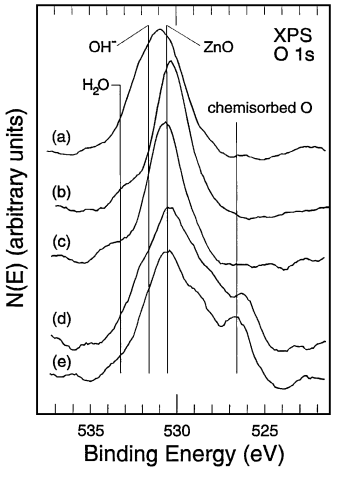

FIG. 7. XPS O 1*s* spectra taken from the 3 wt% K/Zn/Cr spinel catalyst after (a) insertion into the UHV system, (b) pretreatment in 1×10^{-7} Torr of H_2 for 4 hr at 250°C, (c) sputtering for 5 min with 1 keV He^+ and 15 min with 1-keV 1:1 He^+ and Ar^+, (d) the aged 3 wt% K/Zn/Cr spinel catalyst, and (e) the aged catalyst after sputtering for 5 min with 1 keV He^+ and 15 min with a 1-keV 1:1 He^+ and Ar^+ mixture.

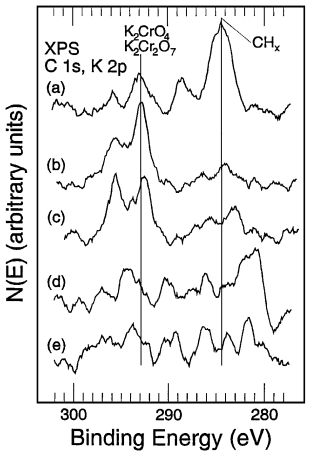

FIG. 8. XPS C 1*s* and K 2*p* spectra taken from the 3 wt% K/Zn/Cr spinel catalyst after (a) insertion into the UHV system, (b) pretreating in 1×10^{-7} Torr of H_2 for 4 hr at 250°C, (c) sputtering for 5 min with 1 keV He^+ and 15 min with a 1-keV 1:1 He^+ and Ar^+ mixture, (d) the aged 3 wt% K/Zn/Cr spinel catalyst, and (e) the aged catalyst after sputtering for 5 min with 1 keV He^+ and 15 min with a 1-keV 1:1 He^+ and Ar^+ mixture.

increased and the hydroxyl group concentration is increased significantly. As shown in Fig. 7e, sputtering does not alter the O 1*s* feature very much indicating that the composition of the near-surface region is fairly uniform with respect to the O species present. The chemisorbed O feature is slightly larger. This is probably due to the sputtering process which could cause the oxides to decompose leading to a greater amount of chemisorbed O.

The XPS C 1*s* spectrum taken from the fresh catalyst is shown in Fig. 8a. The primary feature has a BE of 284.4 eV which is assigned as due to hydrocarbons. These catalysts had been exposed to air which typically results in accumulation of hydrocarbon contamination at the surface. A small K $2p_{3/2}$ peak also is apparent at a BE of 293.0 eV. A previous XPS study of $K_2Cr_2O_7$ has shown that its K $2p_{3/2}$ peak has a BE of 292.8 eV (29), and the BE value of the K $2p_{3/2}$ peak obtained from K_2CrO_4 is 292.6 eV (30). The Cr 2*p* XPS spectrum taken from the fresh catalyst is shown in Fig. 9a. The primary peak has a BE of 579.6 eV which also can be assigned as $K_2Cr_2O_7$ (31, 32). These data indicate that a K–Cr complex exists in the near surface region of the fresh catalyst.

An XPS C 1*s* and K 2*p* spectrum obtained from the reduced catalyst is shown in Fig. 8b. The C 1*s* peak is greatly reduced in size, and the K 2*p* peaks are increased in size. The reductive pretreatment nearly eliminates the carbon contamination in the near-surface region and causes K to migrate toward the surface. Even though XPS is much less surface sensitive than ISS, these data are consistent with the ISS data discussed above which indicate that the outermost surface layer of this sample is composed primarily of K after the pretreatment. The BE values of both the K 2*p* features

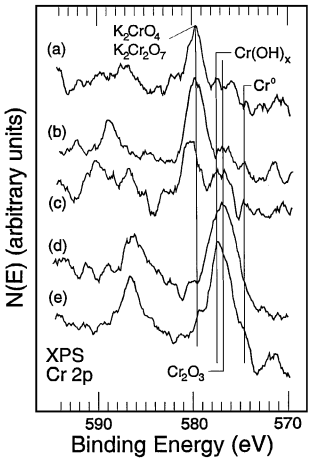

FIG. 9. XPS Cr 2*p* spectra taken from the 3 wt% K/Zn/Cr spinel catalyst after (a) insertion into the UHV system, (b) pretreatment in 1×10^{-7} Torr of H_2 for 4 hr at 250°C, (c) sputtering for 5 min with 1 keV He^+ and 15 min with a 1-keV 1:1 He^+ and Ar^+ mixture, (d) the aged 3 wt% K/Zn/Cr spinel catalyst, and (e) the aged catalyst after sputtering for 5 min with 1 keV He^+ and 15 min with a 1-keV 1:1 He^+ and Ar^+ mixture.

and Cr 2*p* features (Fig. 9b) can be assigned as potassium dichromate or potassium chromate as discussed above. The Cr 2*p* peaks are almost doubled in size due to this treatment also. This increase in the Cr 2*p* peak sizes are apparent in the XPS survey spectrum taken from this sample as well (not shown). The reactivity data shown in Table 1 demonstrate the necessity of K in order to produce isobutanol. The XPS and ISS data both indicate that the K is present at the surface, and the XPS data indicate that it is associated with the Cr after the reductive pretreatment. Furthermore, the XPS data indicate that C and some O contamination is removed by this treatment as well which most likely exposes a greater number of active sites. After sputtering the catalyst with 1 keV He^+ for 5 min and a 1-keV 1:1 He^+ and Ar^+ mixture for 15 min, the spectra shown in Figs. 8c and 9c were taken. The K 2*p* peak is shifted to a lower BE probably due to partial decomposition of the $K_2Cr_2O_7$ or $KCrO_4$. The Cr 2*p* spectrum obtained after sputtering contains features due to the presence of $Cr(OH)_x$, Cr_2O_3 (33), and potassium chromate. The former Cr species form upon decomposition of the potassium chromate or by exposure of Cr in the underlying substrate as the K-containing layer is sputtered away.

A C 1*s* and K 2*p* spectrum taken from the aged catalyst is shown in Fig. 8d. Features due to K and C are no longer apparent before or after sputtering (Fig. 8e). The XPS Cr 2*p* spectrum obtained from the aged catalyst is shown in Fig. 9d. Significant changes in the near surface region have occurred during the reaction process. The predominant peak due to potassium chromate present in the spectra taken from the fresh catalyst is decreased significantly in size. The primary peak is now assigned to Cr_2O_3 and $Cr(OH)_x$, and a small Cr^0 signal is also apparent. Sputtering the aged sample reduces some of the Cr_2O_3 to Cr^0 as shown by comparing Figs. 9d and 9e. $Cr(OH)_x$ species also are exposed which initially are present beneath the outermost surface layers. Although no significant changes in catalytic activity occurred between the beginning and end of the experimental runs, the XPS data indicate that little K is present in the near-surface region of the aged catalyst. However, both K and Na are present according to the ISS data in Fig. 4a. K apparently is depleted by some undetermined mechanism during the reaction, but it is replaced by subsurface Na. Since alkali ions remain on the surface, the catalytic activity does not decay. These surface characterization results indicate that a catalytically active phase for HAS is alkali-promoted ZnO.

CONCLUSIONS

A commercially available Zn/Cr spinel methanol-synthesis catalyst (Englehard Zn-0312) has been promoted with various amounts of K and tested for isobutanol synthesis. The best operating parameters for the 1 and 3 wt% K catalyst are the higher temperature and pressure settings of 440°C and 1500 psig. The total alcohol production rate initially increases upon adding K as does the isobutanol production rate which achieves a maximum with the addition of 1 wt% K. The methanol and hydrocarbon production rates also decrease with increasing K above 1 wt% although the 5 wt% K catalyst does produce a slightly higher amount of methanol than the 3 wt% K catalyst. The use of the 3 wt% K catalyst at 440°C and 1500 psi results in the lowest methanol-to-isobutanol mole ratio of 1.5. An isobutanol production rate as high as 103 g/kg-cat/hr is achieved using the Zn/Cr spinel promoted with 1 wt% K. The near-surface region of the fresh catalyst is found to be composed primarily of ZnO and a small amount of hydrocarbon contamination. Reducing the catalyst at 250°C for 4 hr in 1×10^{-7} Torr of H_2 eliminates the C from the near-surface region and induces the K to cover the ZnO. The K is associated with Cr as potassium chromate or dichromate. The active catalyst sites apparently are alkali ions on ZnO. No Zn/Cr spinel structures were observed at the surface which indicates it only acts as a high-surface-area support. The aged catalyst, which was removed from the reactor after a 5-day test period, contains very little K in the near-surface region according to XPS but a significant amount of both K and Na in the outermost atomic layer according to ISS. The Cr is present as Cr_2O_3, $Cr(OH)_x$ and Cr^0, and K is present as a chromate or dichromate after the reductive pretreatment.

ACKNOWLEDGMENT

Financial support for this research was provided by the National Science Foundation through Grant CTS-9122575 and the Department of Energy through Contract DE-AC22-91PC90046.

REFERENCES

1. Satterfield, C. N., "Heterogeneous Catalysis in Industrial Practice," 2nd ed., p. 454. McGraw–Hill, New York, 1991.
2. SRI PEP Review, "Dow/Union Carbide Process for Mixed Alcohols from Syngas," March 1986.
3. Forzatti, P., Tronconi, E., and Pasquon, I., *Catal. Rev. Sci. Eng.* **33**, 109 (1991).
4. Nunan, J. G., Bogdan, C. E., Klier, K., Smith, K. J., Young, C.-W., and Herman, R. G., *J. Catal.* **116**, 195 (1989).
5. Nunan, J. G., Herman, R. G., and Klier, K., *J. Catal.* **116**, 222 (1989).
6. Smith, K. J., and Anderson, R. B., *Can. J. Chem. Eng.* **61**, 40 (1983).
7. Boz, I., Sahibzada, M., and Metcalfe, I., *Ind. Eng. Chem. Res.* **33**, 2021 (1994).
8. Calverley, E., and Smith, K., *Ind. Eng. Chem. Res.* **31**, 792 (1992).
9. Stiles, A., Chen, F., Harrison, J., Hu, X., Storm, D., and Yang, H., *Ind. Eng. Chem. Res.* **30**, 811 (1991).
10. Kiennemann, A., Idriss, H., Kieffer, R., Chaumette, P., and Durand, D., *Ind. Eng. Chem. Res.* **30**, 1130 (1991).
11. Vedage, G. A., Himelfarb, P. B., Simmons, G. W., and Klier, K., *Am. Chem. Soc. Symp. Ser.* **279**, 295 (1985).
12. Tronconi, E., Ferlazzo, N., Forzatti, P., and Pasquon, I., *Ind. Eng. Chem. Res.* **26**, 2122 (1987).
13. Villa, P. L., DelPiero, G., Cipelli, A., Lietti, L., and Pasquon, I., *Appl. Catal.* **27**, 161 (1986).
14. Forzatti, P., Cristiani, C., Ferlazzo, N., Lietti, L., Tronconi, E., Villa, P. L., and Pasquon, I., *J. Catal.* **111**, 120 (1988).
15. Beretta, A., Sun, Q., Herman, R., and Klier, K., *Ind. Eng. Chem. Res.* **35**, 1534 (1996).
16. Tronconi, E., Lietti, L., Forzatti, P., and Pasquon, I., *Appl. Catal.* **47**, 317 (1989).
17. Wagner, C. D., Riggs, W. M., Davis, L. E., Moulder, J. F., and Muilenberg, G. E., "Handbook of X-Ray Photoelectron Spectroscopy," Perkin–Elmer, Eden Prarie, MN, 1979.
18. Gilbert, R. E., Cox, D. F., and Hoflund, G. B., *Rev. Sci. Instrum.* **53**, 1281 (1982).
19. Young, V. Y., and Hoflund, G. B., *Anal. Chem.* **60**, 269 (1988).
20. Young, V. Y., Hoflund, G. B., and Miller, A. C., *Surf. Sci.* **235**, 60 (1990).
21. Melendez, O., Hoflund, G. B., Gilbert, R. E., and Young, V. Y., *Surf. Sci.* **251/252**, 228 (1991).
22. Young, V. Y., Welcome, N., and Hoflund, G. B., *Phys. Rev. B* **48**, 2891 (1993).
23. Davidson, M. R., Hoflund, G. B., and Outlaw, R. A., *J. Vac. Sci. Technol. A* **9**, 1344 (1991).
24. Gardner, S. D., Hoflund, G. B., and Schryer, D. R., *J. Catal.* **119**, 179 (1989).
25. Barr, T. L., and Hackenberg, J., *Appl. Surf. Sci.* **10**, 523 (1982).
26. Baltistoni, C., Dormann, J. L., Fiorani, D., Paparazzo, E., and Viticoli, S., *Solid State Commun.* **39**, 581 (1981).
27. Weaver, J. F., and Hoflund, G. B., *J. Phys. Chem.* **98**, 8519 (1994).
28. Weaver, J. F., and Hoflund, G. B., *Chem. Mater.* **6**, 1693 (1994).
29. Nefedov, V. I., Salyn, Y. V., Solozhenkin, P. M., and Putatov, G. Y., *Surf. Interface Anal.* **2**, 171 (1980).
30. Allen, G. C., Curtis, M. T., Hooper, A. J., and Tucker, P. M., *J. Chem. Soc. Dalton Trans.* 1677 (1973).
31. Tsutsumi, T., Ikemoto, I., Namikawa, T., and Kuroda, H., *Bull. Chem. Soc. Jpn.* **54**, 913 (1981).
32. Ikemoto, I., Ishii, K., Kinoshita, S., Kuroda, H., Franco, M. A. A., and Thomas, J. M., *J. Solid State Chem.* **17** (1976).
33. Capece, F. M., DiCastro, V., Furlani, C., Mattogno, G., Fragale, C., Gargano, M., and Rossi, M., *J. Electron Spectrosc. Relat.Phenom.* **27**, 119 (1982).